Anal. Chem. **2006,** *78,* 3304−3315

Characterizing the Structures and Folding of Free Proteins Using 2-D Gas-Phase Separations: Observation of Multiple Unfolded Conformers

Alexandre A. Shvartsburg, Fumin Li, Keqi Tang, and Richard D. Smith*

Biological Sciences Division, Pacific Northwest National Laboratory, P.O. Box 999, Richland, Washington 99352

Understanding the 3-D structure and dynamics of proteins and other biological macromolecules in various environments is among the central challenges of chemistry. Electrospray ionization can often transfer ions from solution to gas phase with only limited structural distortion, allowing their profiling using mass spectrometry and other gas-phase approaches. Ion mobility spectrometry (IMS) can separate and characterize macroion conformations with high sensitivity and speed. However, IMS separation power is generally insufficient for full resolution of major structural variants of protein ions and elucidation of their interconversion dynamics. Here we report characterization of macromolecular conformations using field asymmetric waveform IMS (FAIMS) coupled to conventional IMS in conjunction with mass spectrometry. The collisional heating of ions in the electrodynamic funnel trap between FAIMS and IMS stages enables investigating the structural evolution of particular isomeric precursors as a function of the intensity and duration of activation that can be varied over large ranges. These new capabilities are demonstrated for ubiquitin and cytochrome *c*, two common model proteins for structure and folding studies. For nearly all charge states, two-dimensional FAIMS/IMS separations distinguish many more conformations than either FAIMS or IMS alone, including some with very low abundance. For cytochrome *c* in high charge states, we find several abundant "unfolded" isomer series not distinguishable by IMS, possibly corresponding to different "string of beads" geometries. The unfolding of specific ubiquitin conformers selected by FAIMS has been studied by employing their heating in the FAIMS/IMS interface.

The function of proteins, DNA, and other biological macromolecules strongly depends on three-dimensional structure, and conformational changes such as protein denaturation generally result in the loss of bioactivity.[1] Specific protein misfolding has also been shown to cause a qualitatively new activity, underlying neurodegenerative diseases[2−7] that in some cases are apparently propagated by a small amount of misfolded protein (prion).[5−7] Such interests call for more sensitive and specific methods for profiling protein conformations. Established NMR and X-ray approaches can elucidate macromolecular geometries in detail[8,9] but are slow and generally require large quantities of pure protein, which makes these methods unsuited for probing real biological matrixes, where the target species is often a minute component of a complex mixture. The need to identify and quantify a misfolded protein in the presence of a dominant normal conformation, and possibly other isomers, is a particular challenge. Conventional mass spectrometric (MS) methods, e.g., collision-induced fragmentation, are generally insensitive to 3-D structure of proteins and their complexes.[10]

In the past decade, the coupling of ion mobility spectrometry (IMS) to MS, using either electrospray ionization (ESI) or matrix-assisted laser desorption/ionization (MALDI), has enabled low-resolution structural characterization of gas-phase macroions, including proteins,[11−23] DNA,[24,25] and polypeptides.[26,27] These

* To whom correspondence should be addressed. E-mail: rds@pnl.gov.

(1) Petsko, G. A.; Ringe, D. *Protein Structure and Function*; Primers in Biology; Sinauer: Sunderland, MA, 2003.
(2) Kirkitadze, M. D.; Bitan, G.; Teplow, D. B. *J. Neurosci. Res.* **2002**, *69*, 567.
(3) Serpell, L. C.; Berriman, J.; Jakes, R.; Goedert, M.; Crowther, R. A. *Proc. Natl. Acad. Sci. U.S.A.* **2000**, *97*, 4897.
(4) Johnson, R. T.; Gibbs, C. J. *N. Engl. J. Med.* **1998**, *339*, 1994.
(5) Will, R. G.; Ironside, J. W.; Zeidler, M.; Cousens, S. N.; Estibeiro, K.; Alperovitch, A.; Poser, S.; Pocchiari, M.; Hofman, A.; Smith, P. G. *Lancet* **1996**, *347*, 921.
(6) Scott, M. R.; Will, R.; Ironside, J.; Nguyen, H. B.; Tremblay, P.; DeArmond, S. J.; Prusiner, S. B. *Proc. Natl. Acad. Sci. U.S.A.* **1999**, *96*, 15137.
(7) Prusiner, S. B. *Science* **1997**, *278*, 245.
(8) Lopez Garcia, F.; Zahn, R.; Riek, R.; Wuthrich, K. *Proc. Natl. Acad. Sci. U.S.A.* **2000**, *97*, 8334.
(9) Zarembinski, T. I.; Hung, L. W.; Mueller-Dieckmann, H. J.; Kim, K. K.; Yokota, H.; Kim, R.; Kim, S. H. *Proc. Natl. Acad. Sci. U.S.A.* **1998**, *95*, 15189.
(10) Badman, E. R.; Hoaglund-Hyzer, C. S.; Clemmer, D. E. *J. Am. Soc. Mass Spectrom.* **2002**, *13*, 719.
(11) Clemmer, D. E.; Hudgins, R. R.; Jarrold, M. F. *J. Am. Chem. Soc.* **1995**, *117*, 10141.
(12) von Helden, G.; Wyttenbach, T.; Bowers, M. T. *Science* **1995**, *267*, 1483.
(13) Valentine, S. J.; Counterman, A. E.; Clemmer, D. E. *J. Am. Soc. Mass Spectrom.* **1997**, *8*, 954.
(14) Li, J.; Taraszka, J. A.; Counterman, A. E.; Clemmer, D. E. *Int. J. Mass Spectrom.* **1999**, *185/186/187*, 37.
(15) Myung, S.; Badman, E. R.; Lee, Y. J.; Clemmer, D. E. *J. Phys. Chem. A* **2002**, *106*, 9976.
(16) Wyttenbach, T.; Kemper, P. R.; Bowers, M. T. *Int. J. Mass Spectrom.* **2001**, *212*, 13.
(17) Valentine, S. J.; Anderson, J. G.; Ellington, A. D.; Clemmer, D. E. *J. Phys. Chem. B* **1997**, *101*, 3891.
(18) Shelimov, K. B.; Jarrold, M. F. *J. Am. Chem. Soc.* **1996**, *118*, 10313.
(19) Shelimov, K. B.; Clemmer, D. E.; Hudgins, R. R.; Jarrold, M. F. *J. Am. Chem. Soc.* **1997**, *119*, 2240.
(20) Hudgins, R. R.; Woenckhaus, J.; Jarrold, M. F. *Int. J. Mass Spectrom. Ion Processes* **1997**, *165/166*, 497.
(21) Shelimov, K. B.; Jarrold, M. F. *J. Am. Chem. Soc.* **1997**, *119*, 2987.
(22) Bernstein, S. L.; Wyttenbach, T.; Baumketner, A.; Shea, J. E.; Bitan, G.; Teplow, D. B.; Bowers, M. T. *J. Am. Chem. Soc.* **2005**, *127*, 2075.

10.1021/ac060283z CCC: $33.50
Published on Web 04/07/2006

studies have provided insights into the thermodynamics and kinetics of protein unfolding and refolding[18,21] as a function of ion charge state, chemical modification, extent of hydration, and temperature. Early IMS/MS investigations probed model systems, e.g., ubiquitin,[10,13−16] lysozyme,[17] cytochrome *c*,[18−20] BPTI,[19,20] and myoglobin.[21] Recent studies have extended to physiologically consequential misfolding, such as for amyloid β-protein[22] and α-synuclein[23] associated with Alzheimer's[2] and Parkinson's[3] diseases, respectively. Another technique for isomeric ion separations in gases is field asymmetric waveform IMS (FAIMS). While still in infancy, it has already shown utility for protein conformer separation.[28−32] The impact of these gas-phase approaches is greatly elevated by extensive evidence that ESI (and to some extent MALDI) can produce ions that retain key aspects of solution structure. In particular, a strong dependence of protein geometries observed in IMS[14,20] and FAIMS[28] on solution conditions (e.g., pH and solvent composition) shows that gas-phase measurements can reflect solution conformations.

In IMS, a moderate electric field pulls ions through a tube filled with a buffer gas. This process separates different ions by their mobility (K), which can be determined from the time an ion spends traversing a known length (the drift time, t_D). The mobility depends on the orientationally averaged cross section Ω between the ion and gas molecule.[33] For any structure, Ω may be evaluated using trajectory calculations of varied sophistication, ranging from a simple projection approximation[34] to an exact hard-spheres scattering model[35] to accurate molecular dynamics in a realistic potential.[36−38] Comparison of projected and measured values allows extracting structural information from IMS data, which is broadly employed to characterize the isomeric diversity of biomolecules, as well as inorganic clusters.[39] In principle, mobility is a function of E/N, where E is the electric field intensity and N is the gas number density.[33] However, IMS is normally operated in the low-field limit where $K(E) \approx K(0)$.

In FAIMS, a gas flow entraining ions passes through the gap between an electrode pair carrying a waveform that creates a strong oscillatory field $E(t)$ across the gap.[40,41] The waveform is asymmetric; thus, the mean positive and negative E are not equal. When peak E/N (the "dispersion field", DF) exceeds ∼30−50 Td (i.e., above typical IMS values by at least 1 order of magnitude), $K(E)$ deviates from $K(0)$ significantly. Then ion displacements during the positive and negative $E(t)$ segments do not cancel exactly, resulting in a net drift across the gap toward one of the electrodes where ions are neutralized on impact. For a particular species, this drift can be offset by superposing a small dc "compensation voltage" (CV) on the asymmetric waveform.[40] Scanning CV creates a spectrum based on the *difference* between ion mobilities at high and low E, i.e., the mean derivative of $K(E)$.

A limitation of IMS is modest resolving power, $R \leq 170$ for singly charged ions[42,43] ($R = t_D/t_W$, where t_W is the full width of a peak at half-maximum). By comparison, condensed-phase methods such as liquid chromatography and capillary electrophoresis can achieve[44] $R \sim 10^3$. Further, a significant correlation exists between ion mobility and mass (m); i.e., IMS and MS separations are not fully orthogonal.[45,46] This reduces the IMS peak capacity for isomer separations to substantially less than R and limits the specificity of structural characterization. This is particularly a limitation for proteins where IMS peaks are broadened because of a multitude of similar ion conformations.[20] ESI often generates an isomeric mixture of protein ions for a given charge state, while studies of protein folding processes generally require following the behavior of a particular starting conformation (e.g., as a function of time, temperature, charge reduction, or chemical modification). The lack of isomer selectivity for precursor in IMS/MS and MS/IMS/MS experiments has limited the ability to unravel the protein folding pathways and measure associated thermodynamic and kinetic properties.[15,47,48] The resolution of FAIMS[49] ($R \sim 20-30$) is lower than that of IMS, which for isomeric separations is partly compensated by FAIMS generally being more orthogonal to MS than is IMS. Unfortunately, no means to calculate high-field mobilities for polyatomic ions yet exist, and hence, no structural information can currently be deduced directly from FAIMS measurements. Energy loss (EL) experiments[29,30] allow shape estimation for protein conformers distinguished in FAIMS. However, EL measures only the mean of the distribution of cross sections for species present (unlike IMS that yields the whole distribution) and thus cannot reveal or separate different isomers.

(23) Bernstein, S. L.; Liu, D.; Wyttenbach, T.; Bowers, M. T.; Lee, J. C.; Gray, H. B.; Winkler, J. R. *J. Am. Soc. Mass Spectrom.* **2004**, *15*, 1435.
(24) Hoaglund, C. S.; Liu, Y.; Ellington, A. D.; Pagel, M.; Clemmer, D. E. *J. Am. Chem. Soc.* **1997**, *119*, 9051.
(25) Gidden, J.; Bushnell, J. E.; Bowers, M. T. *J. Am. Chem. Soc.* **2001**, *123*, 5610.
(26) Counterman, A. E.; Clemmer, D. E. *J. Am. Chem. Soc.* **2001**, *123*, 1490.
(27) Hartings, M. R.; Kinnear, B. S.; Jarrold, M. F. *J. Am. Chem. Soc.* **2003**, *125*, 3941.
(28) Purves, R. W.; Barnett, D. A.; Guevremont, R. *Int. J. Mass Spectrom.* **2000**, *197*, 163.
(29) Purves, R. W.; Barnett, D. A.; Ells, B.; Guevremont, R. *J. Am. Soc. Mass Spectrom.* **2000**, *11*, 738.
(30) Purves, R. W.; Barnett, D. A.; Ells, B.; Guevremont, R. *J. Am. Soc. Mass Spectrom.* **2001**, *12*, 894.
(31) Robinson, E. W.; Williams, E. R. *J. Am. Soc. Mass Spectrom.* **2005**, *16*, 1427.
(32) Borysik, A. J. H.; Read, P.; Little, D. R.; Bateman, R. H.; Radford, S. E.; Ashcroft, A. E. *Rapid Commun. Mass Spectrom.* **2004**, *18*, 2229.
(33) Mason, E. A.; McDaniel, E. W. *Transport Properties of Ions in Gases*; Wiley: New York, 1988.
(34) von Helden, G.; Hsu, M. T.; Gotts, N.; Bowers, M. T. *J. Phys. Chem.* **1993**, *97*, 8182.
(35) Shvartsburg, A. A.; Jarrold, M. F. *Chem. Phys. Lett.* **1996**, *261*, 86.
(36) Mesleh, M. F.; Hunter, J. M.; Shvartsburg, A. A.; Schatz, G. C.; Jarrold, M. F. *J. Phys. Chem.* **1996**, *100*, 16082.
(37) Shvartsburg, A. A.; Schatz, G. C.; Jarrold, M. F. *J. Chem. Phys.* **1998**, *108*, 2416.
(38) Shvartsburg, A. A.; Liu, B.; Siu, K. W. M.; Ho, K. M. *J. Phys. Chem. A* **2000**, *104*, 6152.
(39) Jackson, K. A.; Horoi, M.; Chaudhuri, I.; Frauenheim, T.; Shvartsburg, A. A. *Phys. Rev. Lett.* **2004**, *93*, 013401.
(40) Purves, R. W.; Guevremont, R.; Day, S.; Pipich, C. W.; Matyjaszczyk, M. S. *Rev. Sci. Instrum.* **1998**, *69*, 4094.
(41) Purves, R. W.; Guevremont, R. *Anal. Chem.* **1999**, *71*, 2346.
(42) Srebalus, C. A.; Li, J.; Marshall, W. S.; Clemmer, D. E. *Anal. Chem.* **1999**, *71*, 3918.
(43) Asbury, G. R.; Hill, H. H. *J. Microcolumn. Sep.* **2000**, *12*, 172.
(44) Shen, Y. F.; Zhang, R.; Moore, R. J.; Kim, J.; Metz, T. O.; Hixson, K. K.; Zhao, R.; Livesay, E. A.; Udseth, H. R.; Smith, R. D. *Anal. Chem.* **2005**, *77*, 3090.
(45) Ruotolo, B. T.; Gillig, K. J.; Stone, E. G.; Russell, D. H. *J. Chromatogr., B* **2002**, *782*, 385.
(46) Shvartsburg, A. A.; Siu, K. W. M.; Clemmer, D. E. *J. Am. Soc. Mass Spectrom.* **2001**, *12*, 885.
(47) Badman, E. R.; Hoaglund-Hyzer, C. S.; Clemmer, D. E. *Anal. Chem.* **2001**, *73*, 6000.
(48) Badman, E. R.; Myung, S.; Clemmer, D. E. *J. Am. Soc. Mass Spectrom.* **2005**, *16*, 1493.
(49) Shvartsburg, A. A.; Tang, K.; Smith, R. D. *J. Am. Soc. Mass Spectrom.* **2005**, *16*, 2.

Additionally, cross sections measured by EL exceed known values by ~20% and cannot be quantitatively related to ion geometries.[29]

The value of a function and its derivative are not correlated a priori. Hence, FAIMS and IMS could be substantially independent, as they are for tryptic peptides.[50] Thus, the resolution and specificity of combined FAIMS/IMS should be superior to those of either FAIMS or IMS alone. Recently, we have coupled FAIMS to IMS for 2-D gas-phase separations (followed by MS) and shown that the separation power of FAIMS/IMS (for peptides) exceeds that of IMS by 1 order of magnitude.[51]

Here we report a FAIMS/IMS study of macromolecular conformations, characterizing ions of bovine ubiquitin—an eukaryotic cytoplasmic protein (76 residues, 8565 Da) extensively probed by IMS,[10,13−16] FAIMS,[28−31] EL,[29,30] H/D exchange,[31,52−55] and electron capture dissociation (ECD).[56] The native structure of ubiquitin involves an α-helix, a short piece of a 3(10)-helix, and a β-sheet containing five strands,[53] allowing rich conformational diversity for a small protein. Lack of disulfide bridges permits facile unfolding of multiply protonated ubiquitin ions driven by Coulomb repulsion.[13,14] Present results show the capability of FAIMS/IMS to map ubiquitin conformers in a 2-D space, resolving more species than either FAIMS or IMS alone. Additionally, heating of FAIMS-separated ions prior to IMS allows tracking the structural evolution of particular isomers. We also present selected FAIMS/IMS data for equine cytochrome *c* (Cyt c)—another common model protein of somewhat larger size (104 residues, 12 384 Da), where all higher charge states exhibit several apparent types of unfolded conformers that are undistinguishable by IMS.

EXPERIMENTAL METHODS

Instrumentation. Experiments were performed using a FAIMS/IMS/TOF MS system described elsewhere.[51] Briefly, the FAIMS Selectra[57] in front of the IMS/MS is electrically floated on the IMS voltage.[51] The two FAIMS electrodes form the coaxial cylinder geometry with a hemispherical end. The gap width is 2.0 mm in the cylindrical part but is adjustable at the terminus (from 1.7 to 2.7 mm) to control the FAIMS resolution.[58] The setting of 2.3−2.5 mm used here provides a reasonable balance between resolution and sensitivity.[51] The asymmetric waveform is bisinusoidal with 750-kHz frequency and optimum 2:1 "high-to-low" ratio.[49] Analyses were performed in the "P2" mode (i.e., using negative DF and CV) appropriate for proteins as C-type ions where $K(E)$ drops with increasing field.[28−31] In general and specifically for ubiquitin,[30] FAIMS performance improves at higher DF levels; we used the maximum of 20 kV/cm allowed in Selectra. Ions from the atmospheric pressure FAIMS are transmitted to the IMS by an ion funnel incorporating a jet disrupter.[59] The funnel, of an "hourglass" design with a large storage volume past the conductance limit for effective ion accumulation,[60] accepts ions from FAIMS stage as a continuous beam and ejects them into IMS drift tube in discrete pulses.

The IMS/MS platform[60,61] comprises a 2.1-m-long modular drift tube and a Q-TOF MS (modified Sciex Q-Star). The drift tube is filled with N_2, with the pressure controlled by a needle valve and monitored using capacitance manometers. The IMS and MS stages are coupled by a 2-in. electrodynamic ion funnel[62] that radially compresses ion packets at the IMS terminus from ~50 to <2 mm in diameter.[61] At ~1−10 Torr, a funnel provides a near-100% ion transmission from IMS to MS over a broad m/z range.[60,61] Importantly, the rf field in the funnel focuses ions to the axis with no measurable effect on axial coordinates[61] and, thus, affects neither the resolution nor the absolute parameters of IMS separation.[60,61] The IMS is coupled to Q-TOF via a differentially pumped quadrupole chamber. The data obtained from TOF detector are processed into 2-D IMS/MS maps.[61]

Experimental Procedure. Ions were generated using a fused-silica nano-ESI emitter[51] with the sample infused at 0.5 μL/min. Droplets are desolvated by N_2 counterflow while pulled into FAIMS by electric field, and another N_2 stream carries ions through FAIMS. The total gas flow was 2 L/min. Since ions are desolvated prior to the FAIMS stage, the inlet capillary (normally the ESI inlet) was not heated. The sample was a 50 μM solution of ubiquitin or cytochrome *c* (Sigma) in 50:49:1 methanol/water/acetic acid, a solvent with high organic content that induces protein denaturation.[14]

The FAIMS CV was scanned at 2−4 V/min, with IMS operated in the continuous transmission regime.[51] Extraction of data at m/z values for desired protein charge state (z) yields a CV spectrum.[28−30] Next, the IMS was switched to normal operation, and a set of IMS/MS maps was generated with the FAIMS stepping[51] through the CV range revealed in spectra for all z with increments of 0.35−1.0 V (mostly 0.35 or 0.5 V). This CV resolution was chosen based on the known peak t_W of ~0.4−1 V for a single species[49,51] and should suffice to capture all conformers. This process yields a dispersion of ions in 3-D FAIMS/IMS/MS space. A cut through this space for a particular m/z creates a 2-D FAIMS/IMS palette presenting isomers for that z. The palette can be further projected onto the IMS or FAIMS axis to produce the corresponding 1-D spectra.

The TOF cycle time is determined by the maximum m/z. The 143-μs period chosen here reveals m/z up to ~2200, which covers $z \geq 4$ for ubiquitin and $z \geq 6$ for Cyt c (i.e., all z generated by ESI). The pressure in IMS was $P = 4.01$ Torr (±0.1%), at $T = 298$ K. A gas flow out of the drift tube toward the ion source that is critical for proper IMS operation was ensured by pressurizing the IMS stage ~0.03 Torr above the inlet ion funnel.[51,61] The IMS pulsing period was 50 ms, resulting in a 2-fold multiplexing of ion packets in the drift tube. Given the range of mobilities for ubiquitin[10,13−16] and Cyt c ions, this modest multiplexing causes

(50) Guevremont, R.; Barnett, D. A.; Purves, R. W.; Vandermey, *J. Anal. Chem.* **2000**, *72*, 4577.
(51) Tang, K.; Li, F.; Shvartsburg, A. A.; Strittmatter, E. F.; Smith, R. D. *Anal. Chem.* **2005**, *77*, 6381.
(52) Cassady, C. J.; Carr, S. R. *J. Mass Spectrom.* **1996**, *31*, 247.
(53) Freitas, M. A.; Hendrickson, C. L.; Emmett, M. R.; Marshall, A. G. *Int. J. Mass Spectrom.* **1999**, *185/186/187*, 565.
(54) Evans, S. E.; Lueck, N.; Marzluff, E. M. *Int. J. Mass Spectrom.* **2003**, *222*, 175.
(55) Geller, O.; Lifschitz, C. *J. Phys. Chem. A* **2005**, *109*, 2217.
(56) Breuker, K.; Oh, H.; Horn, D. M.; Cerda, B. A.; McLafferty, F. W. *J. Am. Chem. Soc.* **2002**, *124*, 6407.
(57) Guevremont, R. *J. Chromatogr., A* **2004**, *1058*, 3.
(58) Guevremont, R.; Thekkadath, G.; Hilton, C. K. *J. Am. Soc. Mass Spectrom.* **2005**, *16*, 948.
(59) Kim, T.; Tang K.; Udseth, H. R.; Smith, R. D. *Anal. Chem.* **2001**, *73*, 4162.
(60) Smith, R. D.; Tang, K.; Shvartsburg, A. A. U.S. Patent 6,818,890, 2004.
(61) Tang, K.; Shvartsburg, A. A.; Lee, H. N.; Prior, D. C.; Buschbach, M. A.; Li, F.; Tolmachev, A. V.; Anderson, G. A.; Smith, R. D. *Anal. Chem.* **2005**, *77*, 3330.
(62) Kim, T.; Tolmachev, A. V.; Harkewicz, R.; Prior, D. C.; Anderson, G. A.; Udseth, H. R.; Smith, R. D.; Bailey, T. H.; Rakov, S.; Futrell, J. H. *Anal. Chem.* **2000**, *72*, 2247.

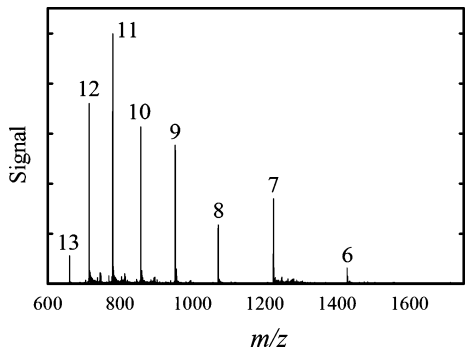

Figure 1. ESI mass spectrum of protonated ubiquitin ions (charge states labeled).

no spatial overlap of different ion packets (as evidenced in the Supporting Information). For maximum IMS resolution, the injection pulse should be shorter than the greater of the diffusional peak width and the detector acquisition window (here the TOF period). Considering the diffusional peak width of ~0.5 ms and TOF period of 0.14 ms, we chose the pulse duration of 0.1 ms. Under these conditions, the IMS resolving power (for $z = 1$) is R ~100 by both calculations and experiment.[61] With resolution limited by diffusion only, R is proportional to $z^{1/2}$; i.e., the theoretical R for ubiquitin ($z = 5-14$) produced by ESI is ~240−400. In reality, the resolution is below the diffusion limit because of finite durations of IMS injection pulse and detector acquisition window,[63] with the theoretical R decreasing to ~220−280. The experimental resolution for protein ion peaks is considerably lower because of unresolved ensembles of (presumably) similar conformers.[14,20]

The rf field in the FAIMS/IMS funnel heats ions during their passage and storage prior to the injection into IMS. The duration of heating may vary from ~1 to ~50 ms depending on the phase of the IMS cycle when ion enters the funnel, but the mean should be <25 ms and perhaps ~10 ms considering some overflow of funnel charge capacity between the IMS pulses that disproportionately depletes ions with longer residence time in the funnel. The heating intensity may be controlled by adjusting the peak rf amplitude U_{rf}, here from 10 to 40 V. The rf ion confinement in the funnel weakens and transmission efficiency starts dropping at $U_{rf} < 20$ V, rendering values below 10 V impractical in the present design. The drift voltage was 3.76 kV, and other voltages were as given previously.[51,61]

RESULTS

In agreement with previous reports,[13,14,16] ESI of ubiquitin from denaturing solution produces a distribution of ion charge states spanning $z = 6-14$ and maximizing at 11+ (Figure 1). The distribution appears bimodal, as observed in some earlier work.[14]

Results of 2-D FAIMS/IMS Separations. The FAIMS spectrum of ubiquitin ions (with any z) spans the CV range of ~ −(6−14) V. The FAIMS/IMS palettes over that range, obtained with minimum ion activation in the front IMS funnel ($U_{rf} = 10$ V), and their projections on two constituent axes are presented in Figure 2; the results for $z = 14$ (not shown) resemble those for 13+. The IMS spectra are consistent with previous findings (for soft ion source conditions and room IMS temperature).[14−16] The protein unfolding induced by charge repulsion starts at 6+ and proceeds through $z = 7-10$ range, where IMS separates "compact", "partially folded", and "elongated" conformation types[13−16] with the fraction of last group increasing from <3% for 6+ and 7+ to ~10% for 8+, ~30% for 9+, and >90% for 10+ (Figure 2). By $z = 11$, the unfolding is complete and further protonation causes no abrupt structural changes.[14,15]

However, the t_D for all $z = 6-14$ are close: Ω increases at higher z (because of unfolding) such that $K(0)$ (proportional to z/Ω) does not change much.[13] The present FAIMS spectra are also consistent with previous results,[28,29] exhibiting two or three features for $z = 6-9$ and a single peak for $z \geq 10$ (the absolute CVs exceed reported values[28,29] because of a higher DF used here: 20 kV/cm versus 16.5 or 17 in earlier work). The present FAIMS/IMS measurements are compared with earlier 1-D separations below.

To correlate the images in 2-D palettes to distinct conformers, we need to gauge the expected 2-D resolution of FAIMS/IMS that defines minimum spot sizes. The apparent R of features in present IMS spectra is 10−22 (Figure 2). Those values are 1 order of magnitude less than the R ~220−280 expected for a single structure (see introduction). This situation in IMS of protein ions is known: the apparent R was ~10−30 for ubiquitin[14] ($z = 6-11$), ~35 for[20] BPTI 5+, and ~10−35 for[20] Cyt c ($z = 8-14$) versus ~350−500 in calculations.[14,20] Evidently, conformations are represented not by single geometries but by ensembles of somewhat differing isomers (e.g., neighboring minimums within a basin on the energy surface). Thus, the maximum observed R of ~20−30 encompasses a typical spread of structures within an ensemble, whereas lower R values indicate a "coelution" of different ensembles in IMS. As FAIMS separates such coeluting ensembles at least in part, peaks in CV-selected IMS spectra are necessarily narrower than those in standard IMS. For example, the values of R for two features for 9+ are 13−18 and 24−25 in FAIMS/IMS (Figure 3) versus 12 and 20, respectively, in IMS (Figure 2). Similar behavior was found for $z = 6-8$. However, the structures within one ensemble should have similar CVs; hence, the $R < 35$ limitation should still apply to CV-selected IMS spectra. Indeed, $R > 35$ was not observed in any spectrum for hundreds of {z; CV} pairs measured here.

The multiplicity of structures within ensemble broadens the peaks in FAIMS spectra as well. The computed t_W of CV features for single ubiquitin geometries under present conditions[64] is ~0.7−0.9 V, and the narrowest peaks in experiment are ~0.8 V wide (for 9+ and 13+, Figure 2). The two values are too close to conclude whether the width is limited instrumentally or by unresolved conformer ensembles—a question to be answered with advances in FAIMS resolution.[49] From FAIMS/IMS data, one could extract t_D-selected FAIMS spectra (analogous to CV-selected IMS spectra in Figure 3). Similarly to the situation in Figure 3, these have peaks that are, on average, narrower than those in common CV spectra, but still with $t_W \geq 0.8$ V. Hence, the effective 2-D FAIMS/IMS resolution may be represented by rectangles spanning ~(2 × 1/35) of t_D (here ~3.5−5 ms for $t_D = 60-90$ ms) along IMS axis and ~(2 × 0.8 V) = 1.6 V along FAIMS axis. (The

(63) Rokushika, S.; Hatano, H.; Baim, M. A.; Hill, H. H., Jr. *Anal. Chem.* **1985**, *57*, 1902.

(64) Shvartsburg, A. A.; Tang, K.; Smith, R. D. *J. Am. Soc. Mass Spectrom.* **2004**, *15*, 1487.

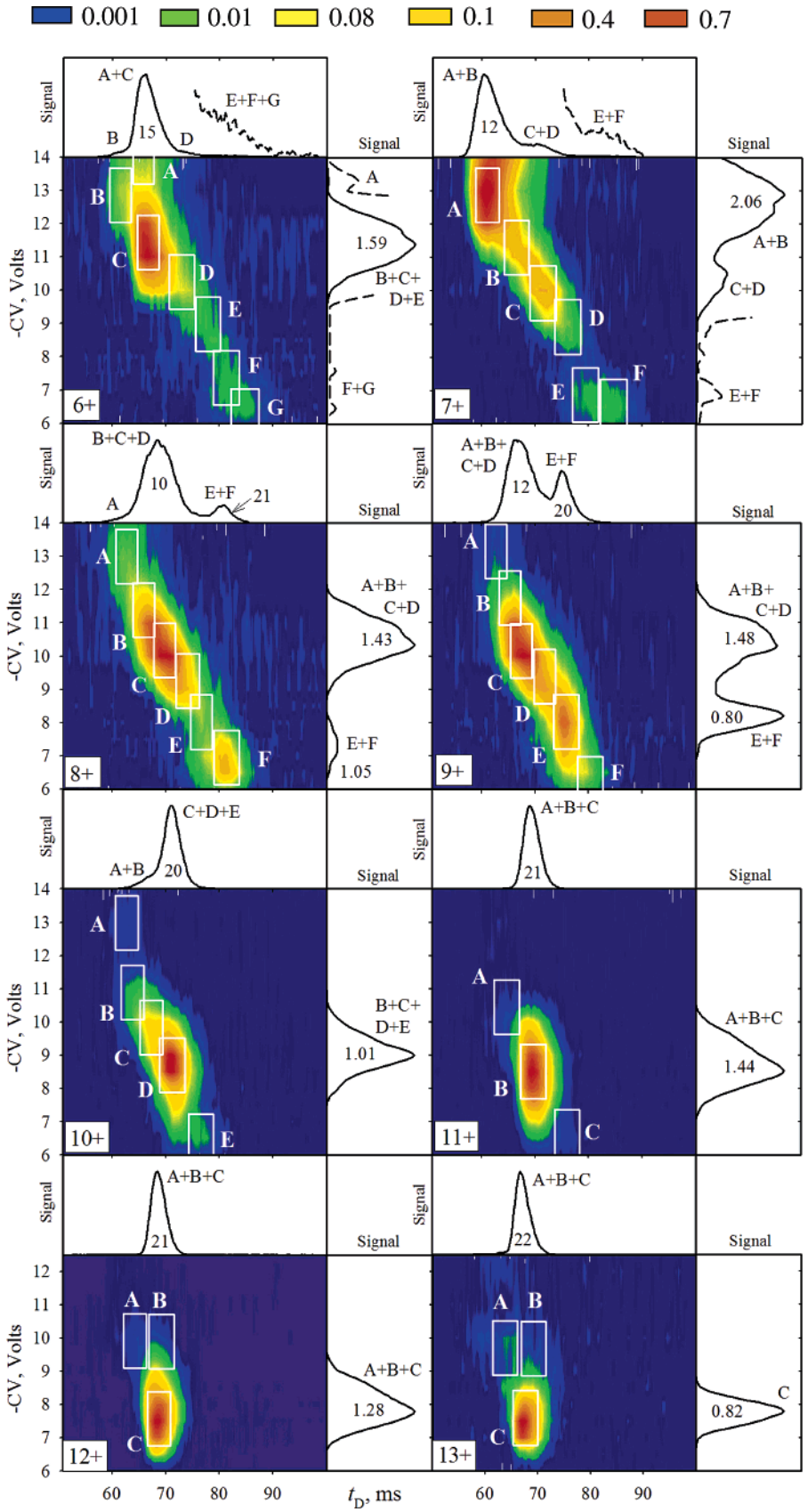

Figure 2. FAIMS/IMS palettes for ubiquitin ions with $z = 6-13$. To the right of each palette is the measured FAIMS CV spectrum (without IMS separation). On top of each palette is the composite IMS spectrum from the projection of palette on the drift time axis. All plots (1-D and 2-D) are scaled to equal dominant peak intensity. In some IMS and FAIMS spectra, small features are magnified 25× (dashed lines). Boxes in palettes (described in the text) define distinct conformers marked in palettes, IMS, and FAIMS spectra by letters. The apparent R for features in IMS spectra and t_W (V) of features in FAIMS spectra are given.

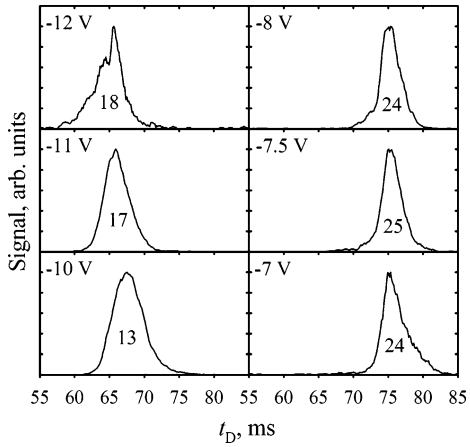

Figure 3. CV-selected IMS spectra for ubiquitin 9+, scaled to equal peak height. The measured IMS resolving power is shown for each feature.

factor of 2 arises from the customary view of a Gaussian distribution as essentially contained within $2t_W$.) Those boxes delineate distinct conformations in palettes (Figure 2), allowing an enumeration of resolved species. Based on IMS resolution for a single structure, each box could contain at least ~10 geometries. Thus, the total number of isomers for gas-phase protein ions of certain charge states (such as $z = 6-8$, Figure 2) may be $>10^2$.

The 2-D palettes for $z = 6-10$ reveal more conformers than IMS or FAIMS spectra individually (Figure 2), e.g., seven distinct spots (A − G) versus three or four peaks in IMS and two or three in FAIMS for 6+. Palettes for $z \geq 11$ exhibit a single major spot, matching the sole peak in IMS or FAIMS. However, trace conformers that are not apparent in palettes may be found in CV-selected IMS spectra. For example, scans at the extremes of CV range for 11+ reveal, in addition to the dominant isomer B, species A and C (Figure 4) parallel to 10+ C and 10+ E, respectively. For 12+ and 13+, minute amounts of isomer A (parallel to the same for 11+) with t_D shorter than that for the major isomer C are seen in IMS scans obtained at the top of CV range (Figure 4), but no conformers with higher t_D (such as 11+ C) were found at any CV. The total counts of species discerned for $z = 6-14$ by FAIMS, IMS, and FAIMS/IMS are listed in Table 1.

The relative abundances of minor isomers are <1% for 12+ and 13+ and ~0.1% for 11+, and all are engulfed by the dominant species in usual IMS (Figure 4). This establishes the dynamic range of $\sim 10^3$ for characterization of isomeric protein mixtures by FAIMS/IMS versus $<10^2$ using IMS.

Conventional IMS often separates isomers not fully but as peak shoulders or tails, precluding reliable determination of t_D. Usually those isomers are fully separated in CV-selected IMS spectra, providing accurate t_D values. For example, IMS indicates unfolded structures for ubiquitin 6+, but does not determine specific t_D (Figure 2), whereas FAIMS/IMS provides t_D values for species E and F (Figure 4). Similarly, IMS indicates the presence of relatively compact minor isomers 8+ A and 10+ B (Figure 2), but accurate t_D could be determined by FAIMS/IMS only (Figure 4). Accurate drift time measurements are critical for correct structural assignments;[35−39] thus, combined FAIMS/IMS should be particularly valuable for structural characterization studies.

Unfolding of Specific Protein Conformers. Structural transitions of selected isomers may be studied using ion heating in the

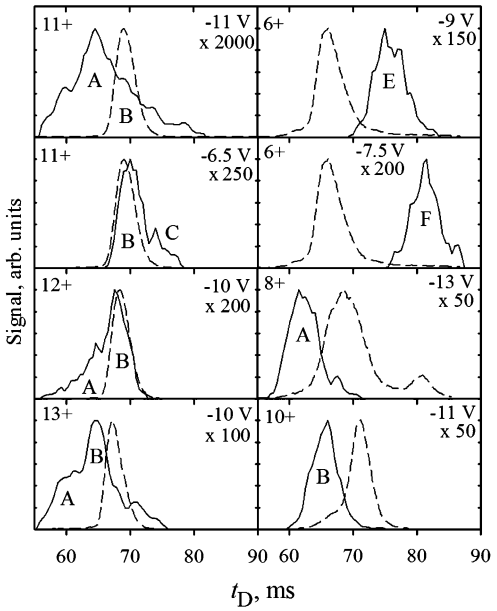

Figure 4. CV-selected IMS spectra (solid lines) revealing trace conformers (left column) and identifying drift times for minor isomers (right column). Standard IMS spectra (dashed lines) are shown for comparison. Plots are scaled to equal peak height; the approximate scaling factors for CV-selected scans are given. Identified species are labeled.

Table 1. Number of Ubiquitin Ion Conformers Distinguished by Ion Mobility Methods (based on Figure 2)

	z									
	6	7	8	9	10	11	12	13	14	all z
IMS	3−4	3	2−3	2	2	1	1	1	1	16−18
FAIMS	2−3	3	2	2	1	1	1	1	1	14−15
FAIMS/IMS	7	6	6	6	5	3	3	3	1	40

FAIMS/IMS funnel. The magnitude of heating ΔT may be estimated using the "two-temperature treatment", where[37]

$$\Delta T = T_{ion} - T = Mv^2/(3k_B) \quad (1)$$

Here T_{ion} and T are the ion and gas temperatures, M is the gas molecule mass, v is the ion velocity, and k_B is the Boltzmann constant. By definition of K, $v = K(E)E(t)$, and $E(t)$ is proportional to U_{rf}. Hence, ΔT in the ion funnel is proportional to $(U_{rf})^2$, and doubling U_{rf} should approximately quadruple ΔT.

Doubling U_{rf} from 10 to 20 V causes new minor conformers to appear in 2-D palettes for $z = 7-9$ (Figure 5) These isomers (7+ A1, 8+ C1, and 9+ C1) have the same CVs as major conformers A and C, respectively, and thus result from their unfolding after FAIMS filtering. The IMS drift time of each new species matches that of the next "more unfolded" major conformer with respect to the parent, 7+ C, 8+ F, and 9+ E, creating a "triangular" pattern. Another doubling of U_{rf} to 40 V causes much greater changes (Figure 5): (i) the abundances of 7+ A1, 8+ C1, and 9+ C1 increase substantially, (ii) new unfolded species appear for $z = 6-10$: B1, C1, and D 1−3 for 6+, A 2−4 and C 1, 2 for 7+, A 1, 2, and B1 for 8+, B1 for 9+, and B1 and C1 for 10+. All

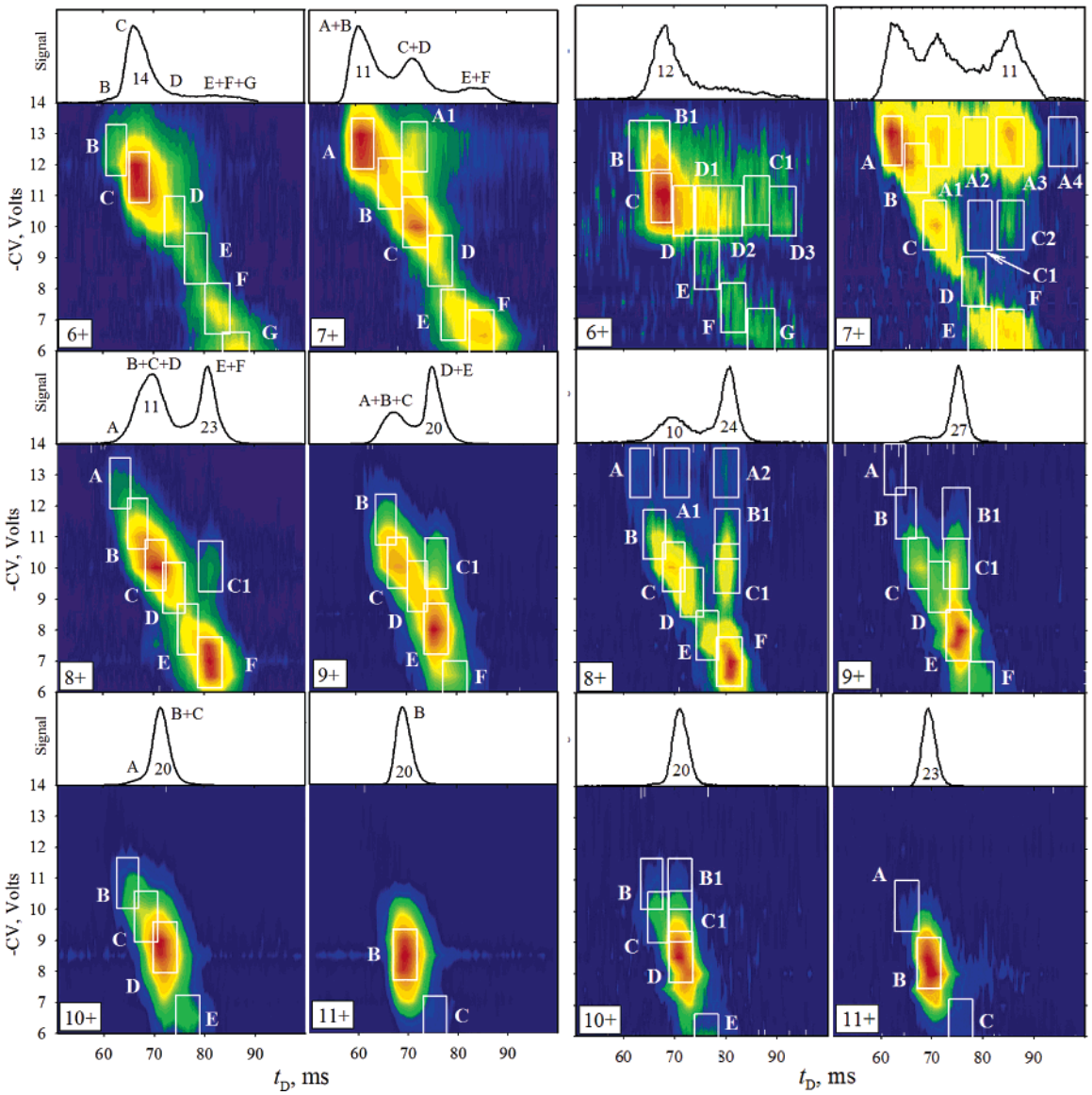

Figure 5. Same as Figure 2 at U_{rf} = 20 (left) and 40 V (right), FAIMS spectra are not shown. The data for 12+ and 13+ are similar to those for 11+.

the new conformers are located to the "right" of a major existing species from which their label is derived. The triangular pattern largely persists, creating the alignments of {A2; C1; E} and {A3; C2; F} for 7+, {A1; C} and {A2; B1; C1; F} for 8+, {B1; C1; E} for 9+, and {B1; C1; D} for 10+. The new (minor) isomers 6+ B1, 6+ D3, and 7+ A4 have no matches at the same t_D values among existing species.

These results mean that heating in the ion funnel pushes a fraction of the conformer population over a barrier to an adjacent major energy basin on the unfolding pathway. As these basins depend on the protein potential energy surface only and not on the activation means, unfolding in the funnel naturally follows the same route as that in the ESI source or ESI/FAIMS interface. However, by probing the isomerization of specific conformers, FAIMS/IMS disentangles the reaction pathways mixed in IMS and thus paints a much more nuanced and quantitative picture of protein unfolding. For example, the unfolding of ubiquitin broadly involves "compact" conformers converting to "partially folded" and on to "elongated" ones,[13,15] e.g., as evident from three peaks for 7+ found in IMS (Figure 5). However, a detailed understanding of relevant thermodynamics and kinetics is obstructed by the coupling between (compact ⇒ partially folded) and (partially folded ⇒ elongated) processes. Decoupling of these reactions in FAIMS/IMS (e.g., replacing {A ⇒ C; C ⇒ F} by {A ⇒ A1; C ⇒ C2} for 7+) enables an accurate measurement of the pertinent properties. This capability would be of particular value for studying the structural evolution of minor isomers. For example, for ubiquitin 8+, IMS provides a reasonable picture of unfolding for the partially folded {B, C, D}, but not for compact conformer A. By removing the interference from major isomers, FAIMS/IMS enables straightforward characterization of such processes, e.g., {A ⇒ A1 ⇒ A2} for 8+ and {B ⇒ B1} for 10+ (Figure 6).

A potential contribution to FAIMS/IMS measurements can arise from charge reduction (e.g., proton transfer) between FAIMS and IMS stages. Proton stripping from highly charged proteins could be effected by some bases such as amines,[52] and nominally endothermic proton transfer can be driven by rf heating in the

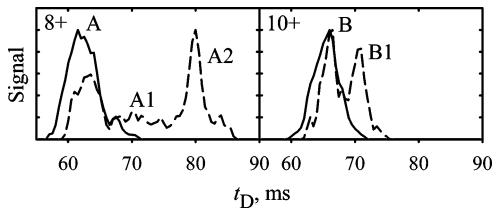

Figure 6. CV-selected IMS spectra at U_{rf} = 10 (solid line) and 40 V (dashed line) show the unfolding of conformers 8+ A (at CV = −13 V, left) and 10+ B (at CV = −11 V, right).

FAIMS/IMS ion funnel. No deprotonation of ubiquitin (even for the highest $z = 15$) was found in previous FAIMS/MS investigations,[30] although those employed a very different post-FAIMS interface with no rf field or extended ion accumulation. Also, ESI-generated protein ions exhibit no charge reduction when injected into IMS in MS/IMS/MS studies[18,19,21] even at energies that induce a complete protein unfolding and thus greatly exceed those used here. The ionization energy (IE) of N_2 buffer gas (15.6 eV) is lower than that of He used in those experiments (24.6 eV), but no proton transfer was found even in the water vapor (IE = 12.6 eV), in agreement with gas-phase basicities of proteins.[65] Deprotonation in the FAIMS/IMS interface would create phantom features with CV of the parent and t_D of the product. Hence, a spot in a 2-D palette for any z cannot result from deprotonation if no spot of substantially higher intensity exists at equal CV for $(z + 1)$. The proton transfer (if any) would be most significant at the highest U_{rf}; hence, we inspected the palettes at $U_{rf} = 40$ V (Figure 5). No spots for 8+ or 9+ have a mirroring spot of higher or even equal intensity at the same CVs for the 9+ and 10+ species, respectively. The sequence of features {8+ E/F, 7+ E/F, 6+ G} (Figures 2 and 5) appears suspicious by this criterion, but 7+ E/F and 6+ G spots are the only ones in the respective palettes at their CVs, and in these cases, corresponding peaks were reported in FAIMS/MS without IMS.[29] Thus, we see no evidence for charge reduction in the FAIMS/IMS interface in present studies but cannot rule out that some trace features might arise from such reactions.

Correlation between FAIMS and IMS Separation Parameters. As with any multidimensional method, the power of FAIMS/IMS and FAIMS/IMS/MS separations depends on the orthogonality of constituent dimensions. The spots in 2-D palettes at low U_{rf} (Figure 2) largely follow decreasing trend lines, evidencing a correlation between the CVs and ion mobilities for protein conformers within most z. This also applies across charge states (Figure 7a), with the r^2 of linear correlation equal to 0.69. However, the values of CV and W are uncorrelated ($r^2 = 0.1$), so CV is not simply a gauge of the degree of protein unfolding (Figure 7b). For example, the fully unfolded major conformers for $z = 10-14$ have higher absolute CVs than some more compact geometries, e.g., 6+ F and 7+ E (Figure 2). The CV and m/z are fully independent (Figure 7c) with $r^2 = 0.00$, meaning that FAIMS/MS would be useful for characterization of protein conformers if a way to obtain structural information from CVs were found.

A substantial correlation between FAIMS and IMS dimensions, if general to protein and macromolecular ions, would be a limitation on their structural characterization using FAIMS/IMS. However, two aspects should be kept in mind. First, unlike in analytical separations such as multidimensional LC, the FAIMS and IMS stages are not equivalent: currently, the conformer structures can only be deduced from the IMS data. This increases the utility of FAIMS/IMS well beyond that suggested by limited independence of FAIMS and IMS dimensions. For example, a 2-D palette containing several spots with equal t_D and different CVs (such as those for Cyt c with $z \geq 13$, below) would exhibit no orthogonality between the two dimensions. From the separation viewpoint, the IMS stage would not contribute to the total peak capacity and therefore would add no value. Of course, that evaluation misses the need for IMS to characterize the separated species. Second, a strong correlation between CV and t_D for particular z allows one to follow the isomerization of individual conformers selected by FAIMS (Figure 5): the existence of multiple species with the same CV but different t_D would preclude choosing a specific precursor for further study. This effectively creates a "tandem IMS" capability—the ion mobility analogue of MS/MS (using Q-TOF instrumentation). That capability could be achieved directly by coupling two IMS stages with isomer selection in the first using a double gate[66] (analogous to a TOF−TOF arrangement). However, the continuous FAIMS filtering offers an important duty cycle/sensitivity advantage over pulsed IMS when individual species are selected in the first stage.

The structures of fragile ions such as proteins may be affected by the FAIMS stage, via field heating, spontaneous unimolecular isomerization, or both over a residence time of 0.2−0.4 s.[67] However, unfolding would generally change the CVs of protein ions by more than the width of FAIMS transmission window (Figures 2 and 5). Hence, structures unfolded inside FAIMS would largely be lost to filtering and thus discriminated against in subsequent IMS data. This "self-cleaning" should reduce the consequences of isomerization in FAIMS, bringing the isomer distributions observed in FAIMS/IMS closer to those produced by ESI (or other ion source). The isomerization of proteins by FAIMS is quantified and will be reported separately.

Absolute Cross Sections and Comparison with Previous Reports. The ion mobilities are obtained from IMS data using[33]

$$K = L^2/(Ut_D) \qquad (2)$$

where L is the drift tube length and U is the voltage across. In principle, IMS/MS measures the ion arrival times that equal t_D plus MS flight times, t_F. We have gauged t_F for present Q-TOF by summing the known flight times through the TOF chamber (~70−120 μs) and estimated transit times through the quadrupoles (~0.2 ms). Though these estimations may be not accurate, the total t_F is <0.6 ms, i.e., <1% of t_D ~60−90 ms under any circumstances. The relative insignificance of t_F in this instrument is confirmed by independence of K from the IMS pressure and drift voltage,[61] and we assumed $t_F = 0$. The drift field in IMS/MS funnel equals that in IMS (~18 V/cm).[51] Therefore, the drift tube

(65) Valentine, S. J.; Clemmer, D. E. *J. Am. Chem. Soc.* **1997**, *119*, 3558.

(66) Sysoev, A.; Adamov, A.; Viidanoja, A.; Ketola, R. A.; Kostiainen, R.; Kotiaho, T. *Rapid Commun. Mass Spectrom.* **2004**, *18*, 3131.

(67) Shvartsburg, A. A.; Tang, K.; Smith, R. D. *J. Am. Soc. Mass Spectrom.* **2005**, *16*, 1447.

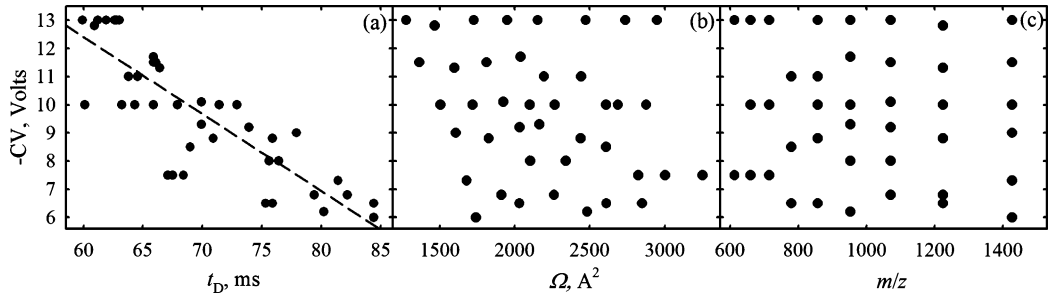

Figure 7. Measured CVs of ubiquitin conformers for $z = 6-14$ (at lowest U_{rf}, Figure 2) vs drift time (a), cross section (b), and m/z (c). The line in (a) is the first-order regression through the data. Panels a and c represent separations in the FAIMS/IMS and FAIMS/MS planes, respectively.

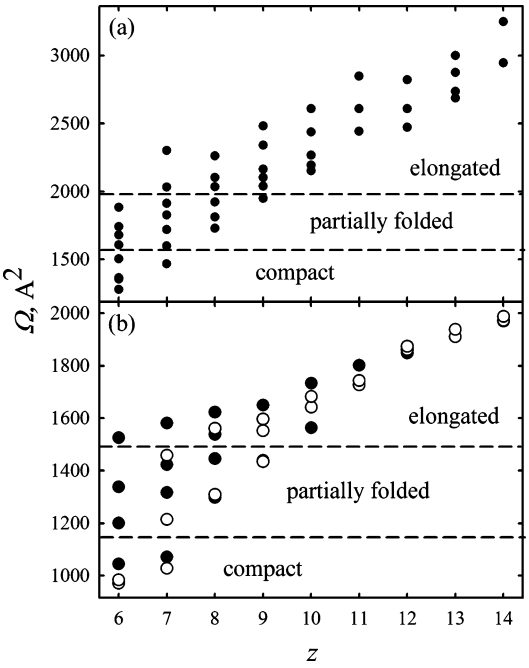

Figure 8. Cross sections of ubiquitin ion conformers as a function of charge state: present measurements including both FAIMS/IMS and direct IMS (a) and previous data (b): from IMS in He gas[13,15] (filled circles) and EL measurements[29,30] in N_2 (empty circles). As previously,[30] values of Ω from EL are scaled such that Ω = 1910 A^2 for one of 13+ isomers. Delineation of structure types is discussed in the text.

and the terminal funnel may be treated as a single unit, and we apply eq 2 with $U = 3.91$ kV and $L = 218$ cm.[51] The values of Ω may be derived from K using the Mason−Schamp equation:[33]

$$\Omega = [3ze/(16N)][2\pi/(\mu kT)]^{1/2}/K \qquad (3)$$

The resulting Ω for all species identified for $z = 6-14$ (at any U_{rf}) are plotted in Figure 8a.

Cross-laboratory comparisons of IMS and FAIMS data for protein ions are complicated by differences of isomeric populations due to source condition variations. Though the Ω in N_2 measured here are naturally higher than those in He[13,16] (by ~30−60%), the overall evolution of Ω for ubiquitin as a function of z (Figure 8a) follows that reported in IMS[13,15] and EL[29,30] studies (Figure 8b). This allows us to designate presently distinguished conformers as compact, partially folded, or elongated using the previous classification based on mobility calculations[13,15] (Figure 8b). For example, for 7+ (Figure 2), A would be compact, F elongated, and B, C, D, and E partially folded. The larger number of isomers found here includes conformers not noted previously, including multiple species for $z = 11-13$. The presence of all these isomers indicates very "soft" conditions in FAIMS and its interfaces, despite a limited annealing due to the rf heating. Based on the data for ubiquitin,[13−16] the present FAIMS/IMS system preserves fragile species at least as well as previous IMS instrumentation.

The cross sections for ubiquitin ions from FAIMS/EL experiments[29,30] also map onto present data well. For 7+, relative Ω for three FAIMS peaks (in the order of increasing absolute CV) were[29] 1:0.85:0.72 versus 1:0.84:0.73 measured here for major species F, C, and A, respectively (Figure 2). However, other conformers were not found by EL. Similarly for 8+, EL produced[29] Ω of 1:0.84 (first at lower absolute CV) for the two peaks separated by FAIMS versus 1:0.85 found here for the dominant species within those peaks (F and C, Figure 2). Again, EL did not reveal other conformers within same FAIMS peaks. For 9+, three isomers with Ω of 1:0.97:0.92 were found, number 1 in the feature at lower absolute CV and numbers 2 and 3 at slightly different CVs within the other feature.[29] The species 1 and 3 match respectively E and C (Figure 2) with Ω of 1:0.90. The isomer 2 has no analogue in Figure 2, but matches C1 (Figure 5) with $\Omega(C1)/\Omega(E) = 0.98$. This suggests some protein unfolding in the FAIMS/EL interface in those experiments,[29] creating new features similar to those in Figure 5 here. For 10+, EL found[29] two isomers with Ω of 1:0.975 (higher Ω at lower absolute CV), possibly corresponding to species D and C (Figure 2) with Ω of ~1:0.95. Concluding, EL provides accurate relative Ω for different species but cannot distinguish multiple isomers in a mixture, even when their presence is indicated by unstable Ω across a FAIMS peak,[29] as for 8+. This fundamentally prevents EL from augmenting FAIMS separations, though it may characterize already separated ions. Not surprisingly, the correlation between CV and Ω in FAIMS/EL study of ubiquitin ions was $r^2 = 0.8$ versus 0.1 found here (Figure 7b).

Multiple Unfolded Conformers for Cytochrome *c*. Like ubiquitin, Cyt c lacks disulfide bridges and is readily unfolded, e.g., by thermal denaturation, multiple charging, or both.[19,20,48,65,68,69] By IMS at low injection energy,[20,65,69] free Cyt c unfolds spontaneously over $z = 9-11$, which is higher than $z = 7-9$ for ubiquitin because of the larger protein size. For the same reason, the ESI MS charge-state envelope for Cyt c spans[11] $z = 7-20$ versus 6−14

(68) Mao, Y.; Ratner, M. A.; Jarrold, M. F. *J. Phys. Chem. B* **1999**, *103*, 10017.
(69) Jarrold, M. F. *Annu. Rev. Phys. Chem.* **2000**, *51*, 179.

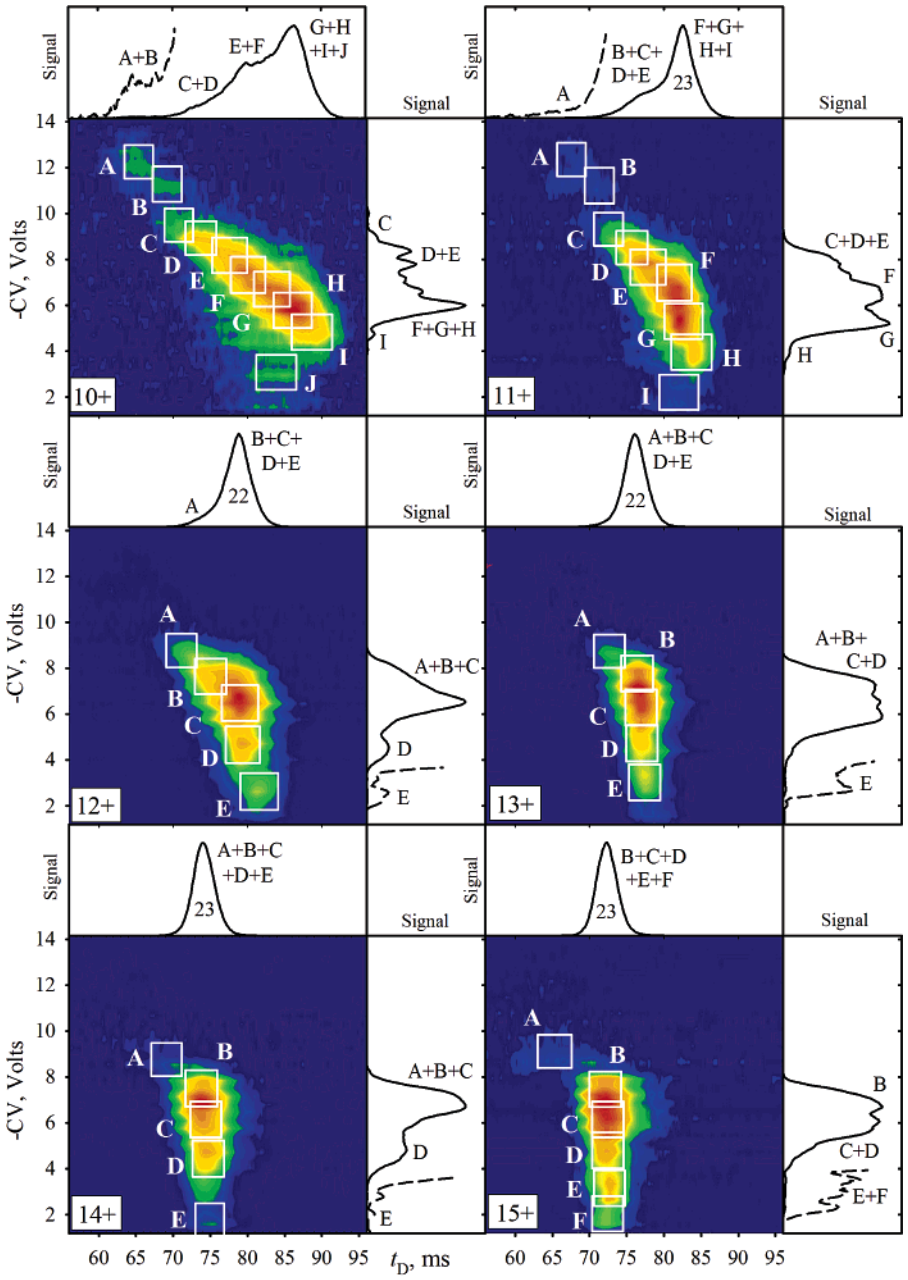

Figure 9. FAIMS/IMS palettes for Cyt c ions with $z = 10-15$. The nomenclature is as in Figure 2. The data for $z = 16-18$ are similar to those for 14+ and 15+.

for ubiquitin. We have acquired the FAIMS/IMS maps for $z = 7-18$ at the intermediate funnel heating level of $U_{rf} = 20$ V (shown in Figure 9 for $z = 10-15$). Unlike in Figure 5 (left panel), no "triangular" pattern appears for any z: apparently Cyt c is more stable to unfolding than ubiquitin, perhaps because of larger protein size. (Compact Cyt c and ubiquitin conformers have very similar mobilities; thus, by eq 1, heating in the funnel at same U_{rf} should be equally intense.) Hence, we need no data at $U_{rf} < 20$ V, where measurements for larger proteins are complicated by lower ion intensity. The projections of 2-D palettes on the IMS axis (Figure 9) reproduce previous findings closely, and the IMS resolving power (for unfolded geometries) is the same $R \sim 20-25$ as for ubiquitin.

A full account of FAIMS/IMS study of Cyt c for all z, including the unfolding of FAIMS-selected precursors at higher U_{rf} (parallel to Figure 5) and absolute Ω values, will be the subject of a future publication. Here we focus on the key novelty: the multiple features in FAIMS spectra and corresponding spots in 2-D palettes for *all* $z = 7-18$. IMS has found several "compact" and "partially folded" Cyt c conformers (representing relatively stable intermediates on the unfolding pathway) for $z \leq 13$ but only a single "unfolded" geometry[20] for greater z. The present FAIMS/IMS data reveal more (up to 10) conformers for $z = 7-12$ but, most importantly, at least three (and likely 4–5) distinct species at virtually equal t_D for each $z = 13-18$ (Figure 9). Some of these have a comparable fractional abundance (e.g., B and C for $z = 13$ or 15), while others may be relatively minor (such as E for $z = 13-15$).

Mobility calculations indicate that the "unfolded" geometries for all $z \leq 20$ are actually not fully unfolded but may resemble a

"string" of solvation shell "beads" surrounding protonated sites connected by short unfolded peptide chains.[19] This geometry type is plausible on a priori energetic grounds, balancing self-solvation of individual charges and minimization of Coulomb forces.[19] However, in general, a number of such string isomers (e.g., with different protonated sites) should be more likely than a uniquely favorable arrangement. Such conformers should have similar Ω and would thus be indistinguishable by IMS (at $R < 35$ achievable for proteins), but could be separated by FAIMS that is normally more sensitive to local variations in ion geometry. This "string theory" appears consistent with the present observation of multiple "unfolded" species for Cyt c in all higher charge states.

While only one major isomer is separated for ubiquitin with $z \geq 11$ here (Figures 2 and 5), broadened FAIMS peaks for 11+ and 12+ suggest coexistence of multiple species. Indeed, four abundant 11+ and 12+ conformers, mapping onto 11+ B and 12+ C spots (Figure 2), were resolved by FAIMS at higher DF.[30] Those species must have equal t_D in IMS and could similarly represent different "string" variants. The reason for this behavior becoming more pronounced for Cyt c may be a greater diversity of "bead" arrangements allowed by longer "strings" (protein backbone), larger number of both "knots for beads" (basic sites) on the "string" and actual "beads" (extra protons), or both. Only one major conformer of ubiquitin 13+ was found in FAIMS previously,[30] and the present peak (Figure 2) has the minimum width appropriate for a single species. Since ubiquitin has 13 basic sites (four arginines, seven lysines, one histidine, and the *N*-terminus), the predominant 13+ species should involve their protonation with little competition from other sites.[52,53] Thus, the presence of only a single major FAIMS feature for ubiquitin 13+ supports the proposition that different strings of beads may have differing protonation sites.

Thorough H/D exchange studies of Cyt c with $z = 10-18$ using FTICR[71−73] have revealed four or five isomeric families with consistent numbers of exchangeable hydrogens in the ~55−135 range. This may tempt one to speculate about possible correlations between the species distinguished by FAIMS and H/D exchange. For example, conformers associated with different protonation sites would explain a relative continuity of H/D exchange patterns[69,72] when Cyt c unfolds with increasing *z*. However, a poor correlation between FAIMS and H/D exchange properties of ubiquitin isomers[31] portends unfavorably for that premise. Also, a combined IMS/H/D exchange study[69] of Cyt c has found only one exchange level for each $z \geq 11$. On the other hand, ubiquitin 13+ exhibits a single level of H/D exchange,[31,53] and those for 12+ are correlated with features distinguished by FAIMS.[31] This issue could be resolved definitively by 3-D FAIMS/IMS/H/D exchange experiments, e.g., using a FAIMS/IMS instrument coupled to FTICR, with IMS in the double-gate mode[66] passing only specific isomer(s) with preset t_D.

CONCLUSIONS AND FUTURE DIRECTIONS

We have demonstrated the structural characterization of gas-phase ions employing 2-D FAIMS/IMS separations in conjunction with mass spectrometry. The capabilities of this new technology were evaluated using ubiquitin and cytochrome *c*, model proteins extensively investigated using IMS, FAIMS, and EL techniques. The overall patterns of protein folding with the charge state increasing from 6+ to 14+ for ubiquitin and from 7+ to 18+ for Cyt c are consistent with previous work. However, for nearly all charge states, FAIMS/IMS distinguishes significantly more conformations than either FAIMS or IMS alone, including some with fractional abundances of ~0.1%. There is a substantial correlation between FAIMS and IMS dimensions that could constitute a limitation of FAIMS/IMS approach. However, that correlation has allowed elucidating the structural evolution of individual conformers in "tandem IMS" experiments where a particular isomer is selected by FAIMS, unfolded by controlled heating in an ion funnel, and the resulting structure is probed by IMS. This capability enables a much more accurate and detailed mapping of macromolecular isomerization pathways and determination of associated thermodynamic and kinetic quantities, especially for minor conformers. Similar tandem IMS experiments may involve fragmentation of ions between FAIMS and IMS by more intense heating or their chemical modification (including charge reduction) by buffer gas additives. For example, one may explore the 3-D structure of the products of dissociation, deprotonation,[52] or hydration[69,73] for specific precursor conformers.

The FAIMS/IMS data for higher charge states of cytochrome *c* ($z = 13-18$) and, to a lesser extent, ubiquitin ($z = 11$ and 12) reveal multiple abundant "unfolded" conformers undistinguishable by IMS alone. Those may be different arrangements of "bead strings" previously hypothesized as likely intermediates on the protein unfolding pathways, possibly associated with competing protonation schemes. We are currently probing this issue further by studying larger proteins such as myoglobin and increasing the peak capacity of FAIMS/IMS through improved FAIMS resolution.

The combination of specificity inherent in 2-D separations with sensitivity provided by ion funnel interfaces makes FAIMS/IMS (in conjunction with MS) a powerful tool for structural characterization of gas-phase ions. The specificity of FAIMS/IMS could be further enhanced by coupling to other gas-phase probes that have proven complementary to either FAIMS or IMS, such as chemical reactivity (e.g., H/D exchange[31,52−55,65,70−72] and deprotonation[52] studies), ECD,[56] and various spectroscopies.[74] For example, deprotonation[52] and H/D exchange[31,52,53] reactions discriminate two ubiquitin 12+ isomers that have a roughly equal abundance and, thus, are likely not species A (or B) and C here (Figure 2) but "coelute" within feature C. However, H/D exchange proceeds on the time scale of ~10−4000 s, i.e., ~$10-10^4$ times longer than FAIMS/IMS separation. Considering that major changes in gas-phase protein structures commonly occur on that time scale, H/D exchange and ion mobility data should be compared with great caution.[31] FAIMS/IMS analyses could also be useful for monitoring the structural evolution of proteins (e.g., in an ion trap), where the peak capacity and specificity of IMS alone have often proven insufficient for deciphering complex time-dependent behaviors.[48]

(70) Suckau, D.; Shi, Y.; Beu, S. C.; Senko, M. W.; Quinn, J. P.; Wampler, F. M.; McLafferty, F. W. *Proc. Natl. Acad. Sci. U.S.A.* **1993**, *90*, 790.
(71) Wood, T. D.; Chorush, R. A.; Wampler, F. M.; Little, D. P.; O'Connor, P. B.; McLafferty, F. W. *Proc. Natl. Acad. Sci. U.S.A.* **1995**, *92*, 2451.
(72) McLafferty, F. W.; Guan, Z.; Haupts, U.; Wood, T. D.; Kelleher, N. L. *J. Am. Chem. Soc.* **1998**, *120*, 4732.
(73) Mao, Y.; Ratner, M. A.; Jarrold, M. F. *J. Am. Chem. Soc.* **2001**, *123*, 6503.
(74) Fromherz, R.; Gantefor, G.; Shvartsburg, *A. A. Phys. Rev. Lett.* **2002**, *89*, 083001.

ACKNOWLEDGMENT

We thank Dr. R. Guevremont and Dr. R. Purves (Ionalytics) for their advice on the use and adaptation of FAIMS systems and for sharing unpublished work; G. Anderson, M. Buschbach, and D. Prior (Pacific Northwest National Laboratory; PNNL) for their critical help with instrumental development; Professor D. E. Clemmer and S. Myung (Indiana) for providing their published IMS data on ubiquitin; and Professor M. T. Bowers (Santa Barbara) and Dr. S. Noskov (Cornell) for valuable discussions. Portions of this work were supported by PNNL Laboratory Directed Research and Development Program and the NIH National Center for Research Resources (RR 18522). PNNL is operated by the Battelle Memorial Institute for the U.S. Department of Energy through contract DE-AC05-76RLO1830.

SUPPORTING INFORMATION AVAILABLE

Additional information as noted in text. This material is available free of charge via the Internet at http://pubs.acs.org.

Received for review February 14, 2006. Accepted March 8, 2006.

AC060283Z